

Effect of roughness on surface boundary conditions for large-eddy simulation

Rob Stoll¹ and Fernando Porté-Agel^{1,2} (fporte@umn.edu)

¹*St. Anthony Falls Laboratory, Department of Civil Engineering, University of Minnesota, Minneapolis, MN 55414, U.S.A.*; ²*National Center for Earth-Surface Dynamics*

Abstract. An important parameterization in large-eddy simulations (LESs) of high-Reynolds-number boundary layers, such as the atmospheric boundary layer, is the specification of the surface boundary condition. Typical boundary conditions compute the fluctuating surface shear stress as a function of the resolved (filtered) velocity at the lowest grid points based on similarity theory. However, these approaches are questionable because they use instantaneous (filtered) variables, while similarity theory is only valid for mean quantities. Three of these formulations are implemented in simulations of a neutral atmospheric boundary layer with different aerodynamic surface roughness. Our results show unrealistic influence of surface roughness on the mean profile, variance and spectra of the resolved velocity near the ground, in contradiction of similarity theory. In addition to similarity-based surface boundary conditions, a recent model developed from an a-priori experimental study is tested and it is shown to yield more realistic independence of the results to changes in surface roughness. The optimum value of the model parameter found in our simulations matches well the value reported in the a-priori wind tunnel study.

Keywords: Aerodynamic surface roughness length, Atmospheric boundary layer, Large-eddy simulation, Surface boundary conditions

1. Introduction

Large-eddy simulation (LES) has become a very useful tool to study turbulent transport of heat, momentum and water vapor in the atmospheric boundary layer (ABL). An important parameterization in LES of high-Reynolds-number boundary layers is the specification of the surface boundary condition. In these flows, the lowest grid points, at which velocity is computed, are located well into the surface (outer) layer and, therefore, the near-surface flow dynamics need to be accounted for through the surface boundary condition. Given the importance of the boundary condition on the dynamics of the flow near the ground, obtaining physically more realistic boundary condition formulations has been recognized as one of the most urgent challenges that needs to be met to make LES a more reliable tool in simulations of high-Reynolds-number boundary layers in both engineering and environmental applications (Cabot and Moin, 2000; Piomelli et al., 1989; Piomelli and Balaras, 2002).



© 2005 Kluwer Academic Publishers. Printed in the Netherlands.

Typical surface boundary conditions for LES consist of specifying the instantaneous local (over an LES grid element) surface shear stress $\tau_{i3,s}(x, y, t)$ (where $i = 1, 2$ denotes the streamwise and spanwise components, respectively, and the subscript s denotes a surface value) at the surface position (x, y) and time t , based on the resolved velocity field at the first vertical grid point. In this study the indices 1,2,3 represent the streamwise (x), spanwise (y) and vertical (z) directions, respectively. A classical model for $\tau_{i3,s}(x, y, t)$, used extensively in LES of high-Reynolds-number boundary layer flows, is (Schumann, 1975; Grötzbach, 1987; Piomelli et al., 1989; Piomelli and Balaras, 2002)

$$\tau_{i3,s}(x, y, t) = \langle \tau_s \rangle \frac{\tilde{u}_i(x, y, z, t)}{U(z)} = -u_*^2 \left[\frac{\tilde{u}_i(x, y, z, t)}{U(z)} \right], \quad (1)$$

where the tilde ($\tilde{}$) denotes the LES filtering operation (Pope, 2000), the angular brackets ($\langle \rangle$) represent a horizontal average, $\tilde{u}_i(x, y, z, t)$ is the instantaneous resolved (filtered) velocity in the i -direction, u_* is the friction velocity, $\langle \tau_s \rangle$ is the mean total surface shear stress (where $\langle \tau_s \rangle$ opposes the fluid momentum and has the sign convention such that $\langle \tau_s \rangle = -u_*^2$), and $U(z)$ is the mean resolved horizontal wind speed at height z (for our case the height of the first grid points). Note that $U(z)$ and u_* are related through the logarithmic law (similarity theory) (Monin and Obukhov, 1954; Kader and Yaglom, 1990)

$$U(z) = \frac{u_*}{\kappa} \left[\ln \left(\frac{z}{z_o} \right) + \Psi_M \right], \quad (2)$$

where z_o is the aerodynamic roughness length, κ is von Kármán constant ($\kappa = 0.4$), and Ψ_M is the stability correction for momentum. Thus, one can write Equation (1) as

$$\tau_{i3,s}(x, y, t) = - \left[\frac{U(z)\kappa}{\ln(z/z_o) + \Psi_M} \right] \left[\frac{\tilde{u}_i(x, y, z, t)\kappa}{\ln(z/z_o) + \Psi_M} \right]. \quad (3)$$

This model will be referred to as the Schumann-Grötzbach (SG) model throughout the rest of the paper.

In simulations of low-Reynolds-number channel flows, Piomelli et al. (1989) applied a surface boundary condition similar to Equation (1). However, to take into account the inclination of the flow structures near the surface, they required that the surface shear stress be correlated to the instantaneous velocity some distance downstream of the point where the surface shear stress is computed. The resulting model is of the form:

$$\tau_{i3,s}(x, y, t) = \langle \tau_s \rangle \frac{\tilde{u}_i(x + \delta_d, y, z, t)}{U(z)}, \quad (4)$$

where δ_d is a displacement in the mean flow direction (assumed to be aligned with the x direction at the surface). The optimum displacement value, obtained from direct numerical simulation (Piomelli et al., 1989) and experimental data (Rajagopalan and Antonia, 1979; Marusic et al., 2001), can be expressed as $\delta_d = z \cot \gamma$, where $8^\circ < \gamma < 13^\circ$ is the typical inclination of flow structures with respect to the surface. The value of γ shows a small dependence on Reynolds number, with the largest values ($\gamma \approx 13^\circ$) corresponding to high-Reynolds-number flows such as the ABL (Piomelli et al., 1989). The model given by Equation (4) will be referred to as the shifted Schumann-Grötzbach (shifted SG) model throughout the rest of the paper.

Both the SG model and the shifted shifted SG model introduced by Piomelli et al. (1989) require knowledge of the mean surface shear stress $\langle \tau_s \rangle$ through either the pressure gradient or the plane averaged wind speed at the first node. A third method, common in LES simulations of shear driven ABLs and, in general, flows where the pressure gradient is unknown or in which no clear homogeneous direction exists, is to use the log-law directly to compute the total resolved surface shear stress at every grid point (Moeng, 1984; Mason and Callen, 1986; Albertson and Parlange, 1999),

$$\tau_s(x, y, t) = - \left[\frac{\tilde{u}_r(x, y, z, t) \kappa}{\ln(z/z_o)} \right]^2. \quad (5)$$

In Equation (5), $\tilde{u}_r(x, y, z, t)$ is the instantaneous resolved velocity magnitude [$\tilde{u}_r(x, y, z, t) = (\tilde{u}_1(x, y, z, t)^2 + \tilde{u}_2(x, y, z, t)^2)^{1/2}$]. The total surface shear stress is then partitioned in the same manner as in Equation (1)

$$\tau_{i3,s}(x, y, t) = \tau_s(x, y, t) \frac{\tilde{u}_i(x, y, z, t)}{\tilde{u}_r(x, y, z, t)}. \quad (6)$$

In the case of homogeneous surface roughness, Equation (6) can be written using Equations (2) and (5) as

$$\tau_{i3,s}(x, y, t) = \langle \tau_s \rangle \frac{\tilde{u}_i(x, y, z, t) \tilde{u}_r(x, y, z, t)}{U(z)^2}. \quad (7)$$

In contrast to the SG and shifted SG models, this model does not guarantee that the average modeled surface shear stress equals the actual mean surface shear stress (even in flows in which the surface shear stress is known a priori through the pressure gradient). It instead relies on the assumption that the instantaneous locally filtered velocity and surface shear stress are in equilibrium. However, the validity of this assumption is questionable unless the computational grid is refined

in the vertical direction so that the aspect ratio of the first grid cell (horizontal to vertical resolution) is much larger than one (Mason and Callen, 1986). Throughout the rest of this paper this model will be referred to as the local SG model.

Note that all the models presented above are based on applying similarity theory to compute the average shear stress (Equations (1) and (4)) or even the fluctuating shear stress (Equation (5)). However, similarity theory was developed using ensemble averages and, therefore, it is not clear that these approaches can reproduce the correct level of fluctuations in the modeled shear stress. Errors in the estimation of those fluctuations are likely to affect the distribution of energy throughout the surface layer and, consequently, in the simulated velocity fields (e.g. turbulence spectra and mean velocity profiles). For example, the non-linear model given by Equations (6) and (7) computes $\tau_{i3,s}$ as proportional to the product $\tilde{u}_i \tilde{u}_r$, with \tilde{u}_r depending on \tilde{u}_i . When used in the numerical solution of the filtered Navier-Stokes equations, this model is expected to produce more damping of the simulated velocity fluctuations near the surface, compared with the linear models given by Equations (1) and (4), where $\tau_{i3,s}$ is linearly related to \tilde{u}_i . Despite this limitation, Equations (1) and (6) are commonly used in simulations of the ABL.

Marusic et al. (2001) carried out a wind tunnel experiment to study the performance of the surface boundary conditions given by Equations (1) and (4). The experimental setup, consisting of an array of x-wire anemometers and shear stress (hot film) sensors, was designed to measure the spatially filtered (resolved in LES) velocity and surface shear stress corresponding to a grid cell in a typical simulation. The modeled surface shear stresses, obtained from the filtered velocities using Equation (1) and Equation (4), were compared to the measured surface shear stress. Results showed that the models clearly under-predict the levels of fluctuations of the stress at all temporal scales. In an attempt to overcome this shortcoming, Marusic et al. (2001) proposed a new model (referred to as MKP model in the rest of the paper) based on the streamwise velocity

$$\tau_{i3,s}(x, y, t) = \langle \tau_s \rangle \frac{\langle \tilde{u}_i(z) \rangle}{U(z)} - \alpha u_* [\tilde{u}_i(x + \delta_d, y, z, t) - \langle \tilde{u}_i(z) \rangle], \quad (8)$$

where $\alpha (= 0.10)$ is a characteristic constant. The new model was chosen so that the modeled shear stress spectrum (calculated from hot-wire sensors at different vertical positions) would match the measured surface shear stress spectrum (from hot-film sensors flush mounted on the smooth wind-tunnel surface) for any position (z) within the logarithmic region. Since the streamwise velocity spectra follow ‘outer-flow’ scaling

(Perry et al., 1986) in the logarithmic layer of both smooth and rough wall boundary layers (Perry et al., 1987), α is expected to have a constant value independent of roughness length (z_o) and Reynolds number. In the a priori study, this model was able to capture the energy levels of the measured surface shear stress better than the traditional model given by Equation (1).

It is important to note that the shifted model given by Equation (4) can be expressed using the new model (Equation (8)) as follows for the streamwise direction (assuming the flow is aligned with the streamwise direction at the surface):

$$\begin{aligned} \tau_{13,s}(x, y, t) &= \langle \tau_s \rangle \frac{\tilde{u}_1(x + \delta_d, y, z, t)}{U(z)} = \\ \langle \tau_s \rangle + \frac{\langle \tau_s \rangle}{U(z)} (\tilde{u}_1(x + \delta_d, y, z, t) - U(z)) &= \\ \langle \tau_s \rangle - \alpha_{eq} u_* [\tilde{u}_1(x + \delta_d, y, z, t) - U(z)], & \quad (9) \end{aligned}$$

where

$$\alpha_{eq} = \frac{\langle \tau_s \rangle}{u_* U(z)} = \frac{\kappa}{[\ln(z/z_o) + \Psi_M]}. \quad (10)$$

From Equation (10), it is clear that α_{eq} is different for different values of z_o and z . This change in the value of α_{eq} with roughness and vertical resolution is inconsistent with the idea that α is a characteristic constant, with little dependence on resolution or surface roughness, as hypothesized by Marusic et al. (2001). A change in the value of α is expected to have an effect on the level of fluctuations of the simulated surface shear stress. In turn, this will affect the resolved turbulent kinetic energy and the mean velocity near the ground through the solution of LES filtered equations.

In this paper we present a series of numerical experiments designed to evaluate the performance of the SG, shifted SG, and local SG boundary conditions in boundary layer simulations and to study the effect of z_o on the simulation results. Also, the boundary condition proposed by Marusic et al. (2001) (MKP model) is tested and the optimum value of the parameter α is determined based on the simulations. This value is compared with the one obtained in the a priori wind tunnel experiment.

2. Numerical Simulations

The SG model, the shifted SG model, the local SG model and the MKP model, all described in section 1, are implemented in simulations of a

neutrally stable (no convective forcing) atmospheric boundary layer. The LES code used is described in Albertson and Parlange (1999) and Porté-Agel et al. (2000). The code solves the filtered Navier-Stokes equations in rotational form (Orszag and Pao, 1974).

The boundary layer is driven by a constant mean streamwise pressure gradient. The simulation domain is divided into $N_x \times N_y \times N_z = 54 \times 54 \times 54$ uniformly spaced grid points and has a vertical extent of $L_z = 1000$ m corresponding to the height of the boundary layer H . The horizontal directions are homogeneous and have dimensions of $L_x = L_y = 2\pi L_z$. They are discretized using pseudo-spectral methods while vertical derivatives are approximated using second order central differences. A staggered grid is used in the vertical direction with vertical grid spacing $\Delta_z = L_z/(N_z - 1)$, resulting in the first horizontal plane of computation at a height of $\Delta_z/2$. The time advancement is second order Adams-Bashforth. Each simulation is run for a long enough time to guarantee that quasi-equilibrium conditions are reached.

Finite differencing in the vertical direction requires boundary conditions to be specified at the top and bottom of the domain. The top boundary uses a stress free condition ($\partial \tilde{u}_1 / \partial z = \partial \tilde{u}_2 / \partial z = 0$). The bottom surface boundary condition is given by one of the models described in section 1. The SG model (Schumann, 1975; Grötzbach, 1987), the shifted SG model (Piomelli et al., 1989) and the local SG model (Moeng, 1984; Mason and Callen, 1986; Albertson and Parlange, 1999) are tested for four different aerodynamic surface roughness lengths $z_o = 0.0001$ m, 0.01 m, 0.1 m and 0.5 m. These roughness lengths are representative of different land surface types, ranging from calm open seas ($z_o \simeq 0.0001$ m) to centers of towns ($z_o \simeq 0.5$ m) (Stull, 1988). The MKP model is also tested using a value of $\alpha = 0.10$ (equal to the value reported by Marusic et al. (2001) in their a priori study). It is important to note that for the MKP model, the normalized quantities presented in the following section (velocity gradient, resolved variance and resolved spectral density) are not affected by different surface roughness length values. Thus, only results corresponding to one value of surface roughness ($z_o = 0.1$ m) are presented in this paper. In both the MKP model and the shifted SG model the value of the filtered velocity $\tilde{u}_i(x + \delta_d, y, z, t)$ is computed by linear interpolation between the two closest values of \tilde{u}_i as suggested by Piomelli et al. (1989). The mean surface shear stress $\langle \tau_s \rangle$, used in the SG, shifted SG and MKP models is calculated by use of the log-law (Equation (2)).

All simulation runs are carried out using the same subgrid-scale (SGS) model: the scale-dependent dynamic model developed by Porté-Agel et al. (2000). This SGS model has the advantage of not requiring the specification of the model coefficient, which is optimized at every

time step based on the dynamics of the resolved scales. Furthermore, this model has been shown to represent the resolved kinetic energy near the surface better than the traditional Smagorinsky (eddy viscosity) model or the standard dynamic model (Porté-Agel et al., 2000), making it well suited for this study of near surface effects.

3. Results

Next, we present results from our simulations with the SG model, the shifted SG model, and the local SG model for different surface roughness lengths ($z_o = 0.0001$ m, 0.01 m, 0.1 m and 0.5 m). These results are compared with those obtained using the MKP Model with $\alpha=0.10$ (the optimum value reported by Marusic et al. (2001)) and $z_o = 0.1$ m. For the normalized resolved flow statistics presented in this section, the MKP model shows no influence of roughness. As shown in section 1, the shifted SG model is a particular case of the MKP model (the case of $\alpha_{eq} = \kappa/[\ln(z/z_o) + \Psi_M]$). Similarly, the SG model is also a particular case of both models (the case of $\delta_d=0$). From Equation (10), an effective parameter α_{eq} can be calculated for the shifted SG model corresponding to each of the roughness lengths under consideration. The resulting values of α_{eq} are shown in Table I. It is important to note that changing the value of the surface roughness in the shifted model is equivalent to changing the value of the parameter in the MKP model. In addition, according to Equation (10), an increase in resolution (decrease in z) has a similar effect on α_{eq} than an increase (by the same factor) in the surface roughness z_o . However, the effect of resolution is expected to be orders of magnitude smaller than the effect of surface roughness for typical values. Note that the maximum rates of change in resolution typically considered in LES studies are within one order of magnitude or less, compared with the almost four orders of magnitude maximum range in surface roughness lengths considered in this study and typical of the ABL. This explains the little sensitivity of our results to changes in resolution (24 x 24 x 24 and 80 x 80 x 80-node simulations were performed (not shown here) in addition to the 54 x 54 x 54-node simulations). Porté-Agel et al. (2000) showed similar little sensitivity of their simulated flow statistics with respect to resolution.

In this paper we present results only for the dominant, stream-wise component of the surface shear stress. Results from the spanwise component show the same qualitative behavior and, therefore, are not presented here. Table II gives a summary of the turbulence statistics (normalized root-mean-square (rms) $\sigma_{\tau_{13,s}}$, skewness and flatness) corresponding to the simulated surface shear stress $\tau_{13,s}$ obtained in our

Table I. Aerodynamic surface roughness length z_o and corresponding effective model parameter α_{eq} from Equation 10.

z_o (m)	0.0001	0.01	0.1	0.5
α_{eq}	0.035	0.059	0.088	0.136

simulations with the SG, shifted SG and local SG models, for the four roughness length values under consideration. Results from the MKP model with $z_o = 0.1$ m are also given for comparison. In addition, the probability density function (pdf) of the fluctuations in the simulated shear stress ($\tau'_{13,s} = \tau_{13,s} - \langle \tau_{13,s} \rangle$) are computed for all cases and plotted in Figure 1. From Figure 1 and Table II, it is clear that the simulated shear stress is non-Gaussian, asymmetric and skewed towards large (in magnitude) shear stress values. For each of the models (except the MKP model, whose results are not affected by roughness), the rms value $\sigma_{\tau_{13,s}}$ increases with roughness length. This effect is more pronounced for the local SG model, for which the skewness of the modeled shear stress increases from a value of 0.881 for $z_o = 0.0001$ m to a value of 1.460 for $z_o = 0.5$ m. Moreover, for any given roughness length, there is a clear effect of the boundary condition formulation on the shape of the pdf. In particular, the surface shear stress obtained with the local SG model has larger skewness and flatness for all roughness length values than the shear stress obtained with the SG or the shifted models (including the MKP model). This result can be explained considering that the local SG model (Equation (7)) computes $\tau_{13,s}$ proportional to $\tilde{u}_1 u_r$ (where u_r is a function of \tilde{u}_1), instead of assuming a simple linear correlation between $\tau_{13,s}$ and \tilde{u}_1 (Equations (1) and (4) for the SG and shifted SG models, respectively). This fundamental difference results in the local SG model weighting extreme shear stress events stronger than the SG or shifted SG models.

In order to study how the different surface boundary conditions affect the resolved velocity field in the surface layer, we begin by examining the mean velocity gradient. The averaged non-dimensional streamwise velocity gradients $\Phi = \kappa z u_*^{-1} dU/dz$ obtained from simulations over the four roughness length values under consideration, using the SG model, the shifted SG model, and the local SG model, are plotted versus the normalized height z/H in Figures 2, 3 and 4, respectively. Similarity theory predicts that Φ will have a constant value of one in the surface layer (lower 10% of the boundary layer) and slightly larger value in the mixed layer (wake layer) above. Furthermore, experimental evidence (Schlichting, 1979; Krogstad et al., 1992; Krogstad

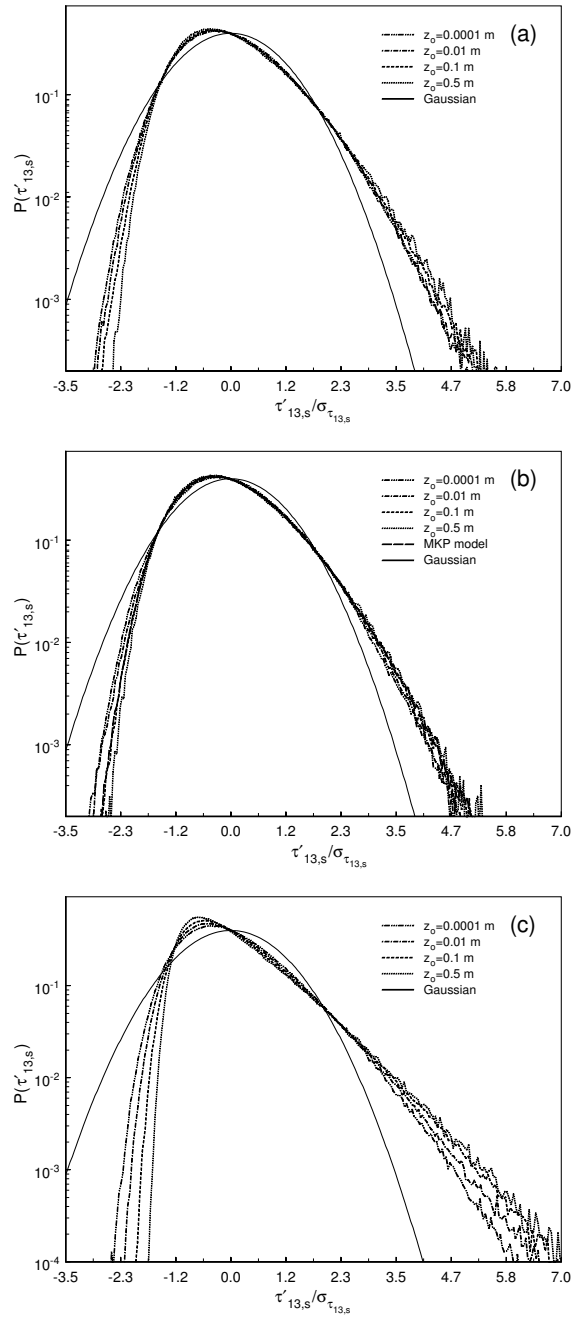


Figure 1. Probability density function of the simulated surface shear stress fluctuations $\tau'_{13,s}$ normalized with its standard deviation and obtained using different surface boundary condition models: (a) SG model, (b) shifted SG model with the MKP model and (c) local SG model. Different lines correspond to different aerodynamic surface roughness lengths. The solid line is the Gaussian distribution with zero mean.

Table II. Statistics of the simulated surface shear stress obtained using different boundary condition formulations over surfaces with the four aerodynamic surface roughness lengths under consideration.

model	z_o (m)	$\sigma_{\tau_{13,s}}$	skewness	flatness
SG	0.0001	0.092	0.576	3.525
	0.01	0.109	0.622	3.545
	0.1	0.213	0.712	3.746
	0.5	0.308	0.810	3.924
shifted SG	0.0001	0.083	0.488	3.346
	0.01	0.125	0.558	3.415
	0.1	0.198	0.642	3.558
	0.5	0.270	0.712	3.670
local SG	0.0001	0.178	0.881	4.230
	0.01	0.268	1.086	4.852
	0.1	0.378	1.314	5.705
	0.5	0.511	1.460	6.135
MKP	0.1	0.201	0.649	3.604

and Antonia, 1999) has shown that for fully rough turbulent boundary layer flows changes in roughness length z_o should only cause a shift in the expected log-law, therefore having no effect on the non-dimensional gradient Φ in the surface layer. In our simulations with the SG model, the shifted SG model and the local SG model, the value of Φ at the lowest levels where the resolved vertical gradient is computed increases with increasing roughness length. The effect is stronger at the lowest level (at $z = \Delta_z$). At that height, Φ ranges from a value of 0.89 for a roughness length z_o of 0.0001 m to a value of 1.17 for z_o of 0.5 m for the SG model, and from a value of 0.86 for z_o of 0.0001 m to a value of 1.09 for z_o of 0.5 m with the shifted SG model. The local SG model shows a similar but less pronounced dependence of Φ with roughness. It increases from a value of 0.96 for a roughness length $z_o = 0.0001$ m to a value of 1.13 for a roughness length of $z_o = 0.5$ m. Note that the clear dependence of Φ on roughness length obtained with the three models is inconsistent with similarity theory. Interestingly, the value of Φ with the shifted SG model is more consistent with similarity theory (closer to a value of one at the first resolved gradient) for the case of $z_o = 0.1$ m. In this case, $\alpha_{eq} = 0.088$, which is very close to the optimum value

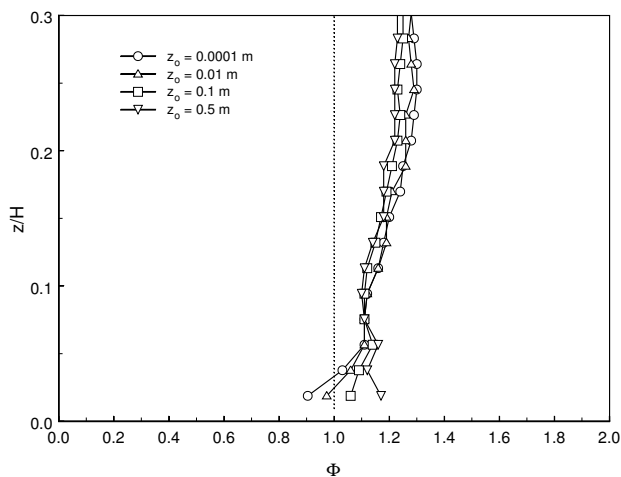


Figure 2. Non-dimensional gradient of the mean streamwise velocity $\Phi = \frac{\kappa z}{u_*} \frac{dU}{dz}$ from simulations that use the SG surface model over surfaces with four different aerodynamic surface roughness lengths z_o . The height z is normalized with the boundary layer depth H . The dotted line corresponds to the classical log-law (expected to hold on the lower 10% of the domain) with $\kappa = 0.4$.

of 0.10 reported by Marusic et al. (2001) (and used here with the MKP model shown in Figure 3).

In order to explore the effect of roughness and boundary condition formulation on the resolved kinetic energy near the ground, the variance of the resolved streamwise velocity (averaged over horizontal planes and over time) is computed and plotted as a function of normalized height in Figures 5, 6 and 7 for the SG, shifted SG and local SG models, respectively. In all three figures it is clear that an increase in roughness is associated with a decrease in the resolved velocity variance at the first vertical grid points where the horizontal velocity is computed ($z = \Delta z/2$). This can be explained by the fact that increasing z_o is associated with increasing fluctuations in $\tau_{13,s}$ as shown in Table II and Figure 1. The increased magnitude of the large shear stress events translates into a stronger damping of the fluctuations of the resolved velocity through the solution of the filtered Navier-Stokes equations. This effect, in turn, is associated with a reduction of the ‘mixing strength’ of the turbulence, which is consistent with the increase in the mean velocity gradient shown in Figures 2, 3 and 4. The roughness effects on the velocity variance is mainly restricted to the lowest computational grid points, above which the resolved kinetic energy shows small dependence on the values of z_o . This observation is in good agreement with previous results

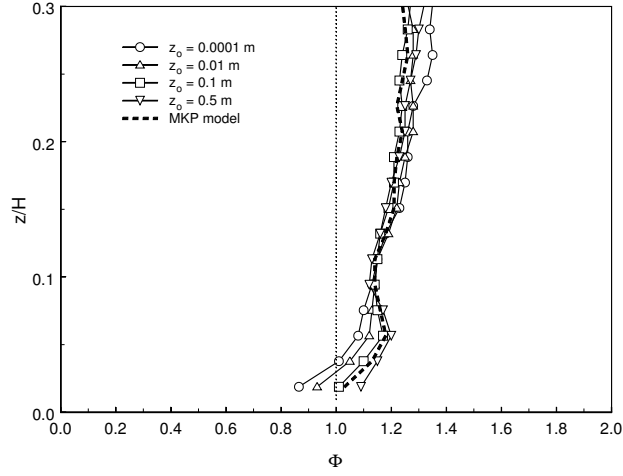


Figure 3. Non-dimensional gradient of the mean streamwise velocity $\Phi = \frac{\kappa z}{u_*} \frac{dU}{dz}$ from simulations that use the shifted SG surface model over surfaces with four different aerodynamic surface roughness lengths z_o . The height z is normalized with the boundary layer depth H . The dashed line corresponds to the MKP model and a surface roughness $z_o = 0.1$ m. The dotted line corresponds to the classical log-law (expected to hold on the lower 10% of the domain) with $\kappa = 0.4$.

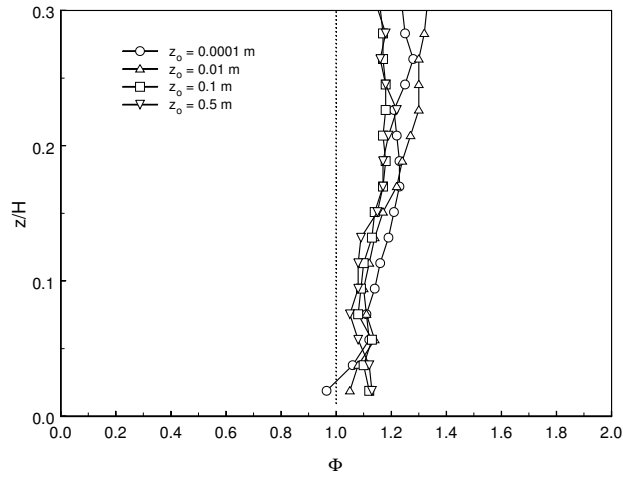


Figure 4. Non-dimensional gradient of the mean streamwise velocity $\Phi = \frac{\kappa z}{u_*} \frac{dU}{dz}$ from simulations that use the local SG surface model over surfaces with four different aerodynamic surface roughness lengths z_o . The height z is normalized with the boundary layer depth H . The dotted line corresponds to the classical log-law (expected to hold on the lower 10% of the domain) with $\kappa = 0.4$.

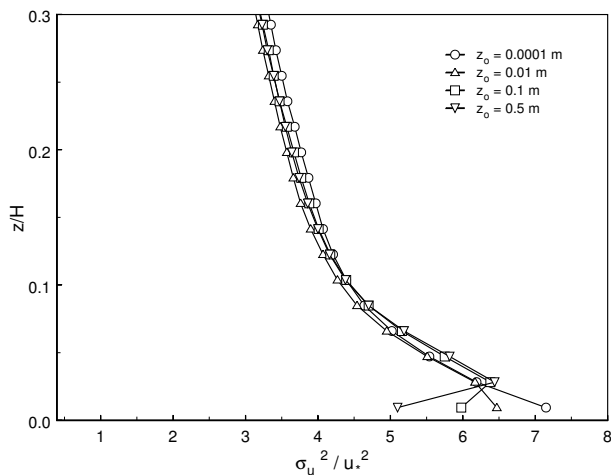


Figure 5. Vertical distribution of the normalized variance of the resolved streamwise velocity from simulations using the SG surface model over surfaces with four different aerodynamic surface roughness lengths z_0 . The height z is normalized with the boundary layer depth H .

from a numerical study of low-Reynolds-number channel flows (Piomelli et al., 1989) showing that boundary condition effects are restricted to the lowest levels of computation.

Next, we study the effect of roughness length on the distribution of the simulated kinetic energy as a function of scale by analyzing the streamwise velocity spectra computed at different heights for the shifted SG model and the local SG model. In a neutrally stable ABL there is experimental evidence that the streamwise velocity energy spectrum is proportional to $k_1^{-5/3}$ at wavenumbers $k_1 \geq z^{-1}$, where z is the measurement height and k_1 is the streamwise wavenumber. These results are consistent with the idea that the flow exhibits local isotropy at the small scales (Kolmogorov, 1941; Saddoughi and Veeravalli, 1994). For smaller wavenumbers ($H^{-1} \leq k_1 \leq z^{-1}$) corresponding to large-scale motions (Kader, 1984; Kader and Yaglom, 1991; Katul et al., 1995; Katul and Chu, 1998), the spectrum is proportional to k_1^{-1} . Furthermore, the change from k_1^{-1} to $k_1^{-5/3}$ scaling is expected to occur near $k_1 z = 1$ and the properly scaled spectra are expected to collapse at scales smaller than the integral scale (H) for all heights in the surface layer (Perry et al., 1986). The normalized streamwise energy spectrum at different levels for the shifted SG model and the local SG model are shown in Figure 8 and 9 each with all the four tested roughness lengths. Spectra are calculated from one-dimensional

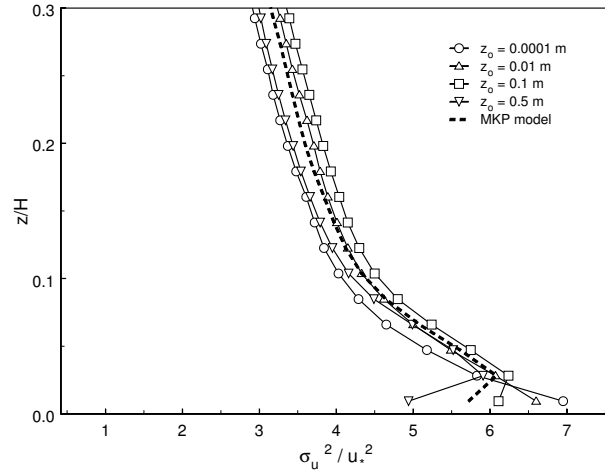


Figure 6. Vertical distribution of the normalized variance of the resolved streamwise velocity from simulations using the shifted SG surface model over surfaces with four different aerodynamic surface roughness lengths z_o . The dashed line corresponds to the MKP model and a surface roughness $z_o = 0.1$ m. The height z is normalized with the boundary layer depth H .

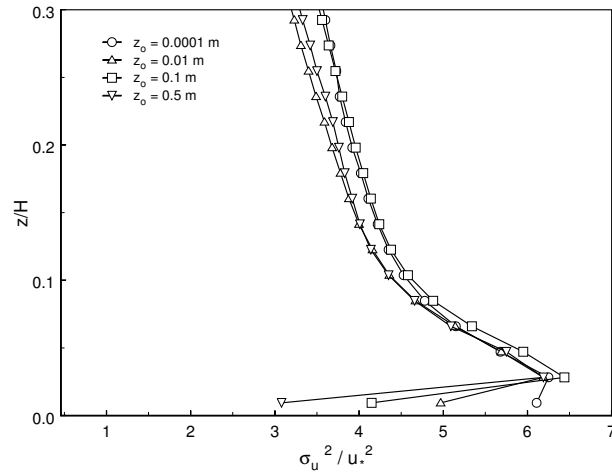


Figure 7. Vertical distribution of the normalized variance of the resolved streamwise velocity from simulations using the local SG surface model over surfaces with four different aerodynamic surface roughness lengths z_o . The height z is normalized with the boundary layer depth H .

Fourier transforms of the streamwise velocity and are then averaged both horizontally and in time. For the lowest levels of computation with the shifted SG model, the spectra shown in Figure 8 exhibit a decrease in energy with increasing roughness values. For a roughness length $z_o = 0.0001$ m, shown in Figure 8(a), the spectrum at the first level $\xi = z/H = 0.009$ is too high and does not show the expected collapse with the closest levels of computation to k^{-1} scaling. With increasing roughness the first level spectra decrease and at $z_o = 0.1$ m, shown in Figure 8(c), the spectrum collapses fairly well for $k_1 z \geq 10^{-1}$. The trend continues and at the largest roughness length tested $z_o = 0.5$ m, the first level spectrum decays to quickly and unrealistically dips below the adjacent energy levels. This observed trend in the spectra with changing roughness is consistent with the trends shown in Figures 3 and 6 for the velocity variance and the normalized velocity gradient. The effects of the surface model on the spectra are confined to the first two levels of computation in all cases and only the largest tested roughness of $z_o = 0.5$ m in Figure 8 (d) shows noticeable effects of the boundary condition at $\xi = 0.028$. This is consistent with the findings in Figures 5 and 6 where the roughness effects on variance are confined to the first level. As for the case of the non-dimensional gradients, the spectral results are more realistic for the case of $z_o = 0.1$ m ($\alpha_{eq} = 0.088$). The spectra shown in Figure 9 for the local SG model have the same general trend of decreasing energy with increasing z_o as the shifted SG model does. In fact, the effect of the surface roughness on the local SG model spectra is even more pronounced than for the shifted SG model. Only the smallest roughness length of $z_o = 0.0001$ m shows the expected collapse towards k^{-1} scaling at the first grid level $\xi = 0.009$. All of the roughness lengths larger than $z_o = 0.0001$ m result in the spectra at the first levels dropping unrealistically below the second levels ($\xi = 0.028$) and for $z_o = 0.5$ m the effect is so strong that it clearly propagates into the second level of computation. This trend of decreasing spectra with increasing surface roughness in the local SG model is consistent with Figures 4 and 7 for the velocity variance and the resolved velocity gradient.

Of special interest is the relation between our simulation results and the findings of Marusic et al. (2001) in their a priori wind tunnel experiment. The effect of changing roughness (z_o) on the results from the SG model or the shifted SG model is equivalent to changing the value of the parameter α in the MKP model. This is inconsistent with the idea that α is independent of roughness and can help understand the shortcomings of both the SG and shifted SG models. It is important to note that the best simulation results are obtained when $\alpha_{eq} \approx 0.10$, which is the same value reported by Marusic et al. (2001). Their study

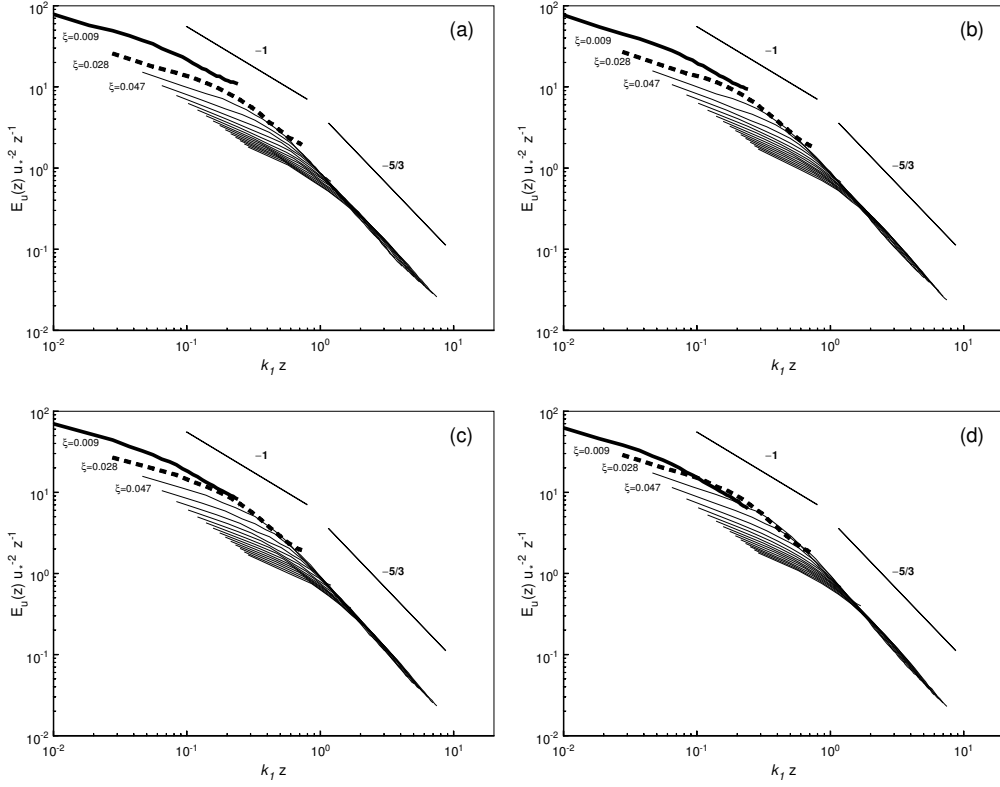


Figure 8. Normalized streamwise velocity spectra at different heights $\xi = z/H$ from simulations with the shifted SG model over surfaces with different aerodynamic surface roughness lengths: (a) $z_o = 0.0001$ m, (b) $z_o = 0.01$ m, (c) $z_o = 0.1$ m and (d) $z_o = 0.5$ m. The thick solid and dashed lines correspond to the first and second levels of computation at $\xi = 0.009$ and $\xi = 0.028$, respectively.

was conducted in a wind tunnel with a smooth surface, and velocity measurements taken at a height z such that $z/z_o \sim 1000$. From Equation (10) this corresponds to a value of $\alpha_{eq} \sim 0.05$. The relatively small value of α_{eq} explains why in their study the modeled surface shear stress computed using both the SG and the shifted SG formulations underestimated the levels of fluctuations in the surface shear stress.

4. Conclusions

A series of numerical experiments are carried out to evaluate the performance of different surface boundary condition formulations in LES of the atmospheric boundary layer, and to study the effect of aerodynamic surface roughness length z_o on the simulation results. Four boundary

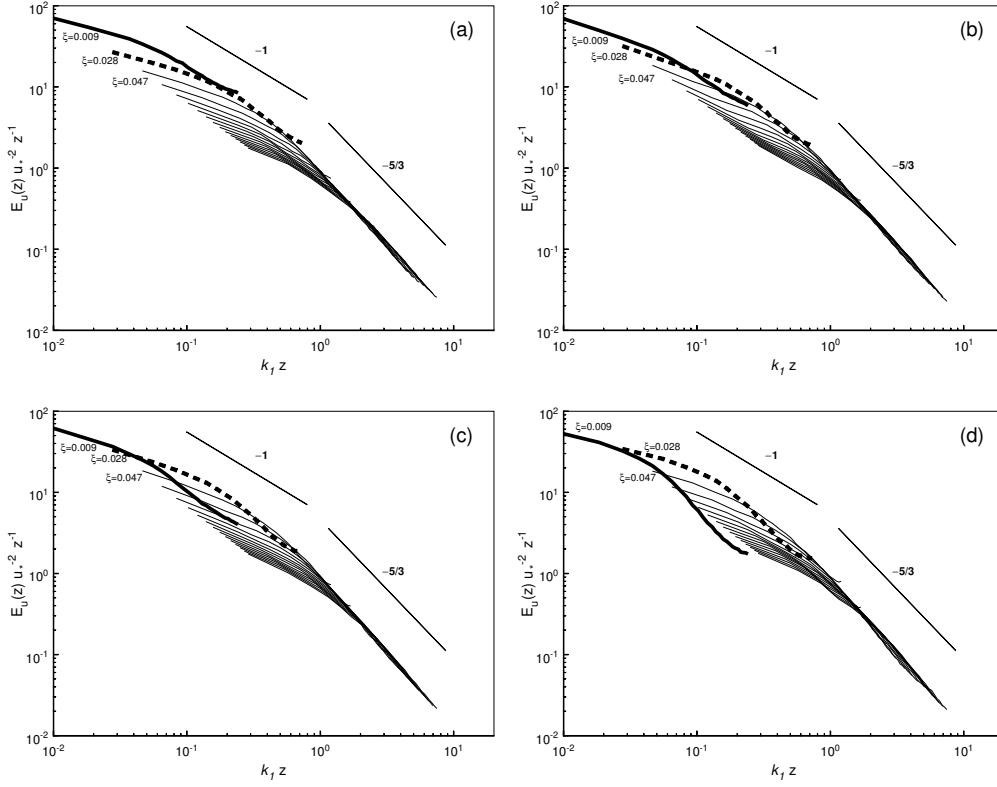


Figure 9. Normalized streamwise velocity spectra at different heights $\xi = z/H$ from simulations with the local SG model over surfaces with different aerodynamic surface roughness lengths: (a) $z_o = 0.0001$ m, (b) $z_o = 0.01$ m, (c) $z_o = 0.1$ m and (d) $z_o = 0.5$ m. The thick solid and dashed lines correspond to the first and second levels of computation at $\xi = 0.009$ and $\xi = 0.028$, respectively.

conditions are studied: the Schumann-Grötzbach (SG) model (Schumann, 1975; Grötzbach, 1987), the shifted SG model (Piomelli et al., 1989), the local SG model (Moeng, 1984; Mason and Callen, 1986; Albertson and Parlange, 1999), and the MKP model recently developed by Marusic et al. (2001) from analysis of wind tunnel data. These boundary conditions are used in simulations of neutral boundary layers over surfaces with different roughness lengths $z_o = 0.0001$ m, 0.01 m, 0.1 m and 0.5 m.

The simulation results show that the SG model, the shifted SG model and the local SG model all yield unrealistic influence of roughness on velocity gradients and energy spectra near the ground, in contradiction of similarity theory and experimental evidence. It is also shown that changing values of roughness z_o in the SG model or the shifted SG

model is analogous to changing α in the MKP model. This is inconsistent with the idea that α is a characteristic parameter that should not be affected by changes in surface roughness, and it provides insight on the reasons for the dependence of the simulation results on surface roughness. In particular, larger values of the roughness length are associated with higher values of the corresponding α_{eq} , which translates into a stronger damping of velocity fluctuations near the surface and, consequently, lower levels of resolved velocity variance and spectra, and larger values of the non-dimensional velocity gradients Φ .

The MKP model with a fixed α gives velocity gradients and spectra that are more realistic and independent of surface roughness. Our simulations also show that for an optimum value of $\alpha \approx 0.10$ streamwise velocity spectra have the correct behavior near the surface: a slope of -1 in the energy production subrange ($kz \lesssim 1$) and a good collapse of the normalized spectra obtained at different heights z . Moreover, the non-dimensional vertical gradient of the average streamwise velocity, Φ , has a value close to one at the first grid point where the velocity gradient is computed. The optimum value of the model parameter $\alpha \approx 0.10$ is in good agreement with the value obtained by Marusic et al. (2001) by matching the energy levels of the modeled and the measured filtered surface shear stress in their wind tunnel study. Our results also show that the effects of the surface boundary condition on turbulence levels and mean velocity gradients are confined to the lowest levels of computation. Due to the large mean shear at those levels, this effect can also introduce significant bias in the simulated mean velocity profiles away from the surface.

Acknowledgements

The authors gratefully acknowledge funding from NSF (grant EAR-0094200) and NASA (grants NAG5-10569 and NAG5-11801). RS was partially supported by a NASA Earth System Sciences fellowship (training grant NNG04GR23H). Computing resources were provided by the University of Minnesota Supercomputing Institute.

References

- Albertson, J. D. and M. B. Parlange: 1999, ‘Surface Length Scales and Shear Stress: Implications for Land-Atmosphere Interactions Over Complex Terrain’. *Water Resources Res.* **35**, 2121–2132.

- Cabot, W. and P. Moin: 2000, ‘Approximate Wall Boundary Conditions in the Large-Eddy Simulation of High Reynolds Number Flow’. *Flow, Turbul. Combust.* **63**, 269–291.
- Grötzbach, G.: 1987, ‘Direct Numerical and Large Eddy Simulations of Turbulent Channel Flows’. In: N. P. Chieremisinoff (ed.): *Encyclopedia of Fluid Mechanics*, Vol. 6. Gulf, pp. 1337–1391.
- Kader, B. A.: 1984, ‘Structure of Anisotropic Velocity and Temperature Fluctuations in a Developed Turbulent Boundary Layer’. *Izv. Akad. Nauk SSSR, Meckh. Zhidk. i Gaza* **4**, 47–56.
- Kader, B. A. and A. M. Yaglom: 1990, ‘Mean Fields and Fluctuation Moments in Unstably Stratified Turbulent Boundary Layers’. *J. Fluid Mech.* **212**, 637–662.
- Kader, B. A. and A. M. Yaglom: 1991, ‘Spectra and Correlation Functions of Surface Layer Atmospheric Turbulence in Unstable Thermal Stratification’. In: O. Métais and M. Lesieur (eds.): *Turbulence and Coherent Structures*. Kluwer.
- Katul, G. G. and R. C. Chu: 1998, ‘A Theoretical and Experimental Investigation of Energy-Containing Scales in the Dynamic Sublayer of Boundary-Layer Flows’. *Boundary-Layer Meteorol.* **86**, 279–312.
- Katul, G. G., R. C. Chu, M. B. Parlange, J. D. Albertson, and T. A. Ortenburger: 1995, ‘Low-Wavenumber Spectral Characteristics of Velocity and Temperature in the Atmospheric Boundary Layer’. *J. Geophys. Res.* **100**, 14243–14255.
- Kolmogorov, A. N.: 1941, ‘The Local Structure of Turbulence in Incompressible Viscous Fluid for Very Large Reynolds Number’. *Dokl. Akad. Nauk S.S.S.R.* **30**, 299–303.
- Krogstad, P. A. and R. A. Antonia: 1999, ‘Surface Roughness Effects in Turbulent Boundary Layers’. *Exp. Fluids* **27**, 450–460.
- Krogstad, P. A., R. A. Antonia, and L. W. B. Browne: 1992, ‘Comparison Between Rough- and Smooth-wall Turbulent Boundary Layers’. *J. Fluid Mech.* **245**, 599–617.
- Marusic, I., G. J. Kunkel, and F. Porté-Agel: 2001, ‘Experimental Study of Wall Boundary Conditions for Large Eddy Simulation’. *J. Fluid Mech.* **446**, 309–320.
- Mason, P. J. and N. S. Callen: 1986, ‘On the Magnitude of the Subgrid-Scale Eddy Coefficient in Large-Eddy Simulations of Turbulent Channel Flow’. *J. Fluid Mech.* **162**, 439–462.
- Moeng, C. H.: 1984, ‘A Large-Eddy Simulation Model for the Study of Planetary Boundary-Layer Turbulence’. *J. Atmos. Sci.* **46**, 2311–2330.
- Monin, A. S. and A. M. Obukhov: 1954, ‘Basic Laws of Turbulent Mixing in the Ground Layer of the Atmosphere’. *Trans. Geophys. Inst. Akad. Nauk. USSR* **151**, 163–187.
- Orszag, S. A. and Y. H. Pao: 1974, ‘Numerical Computation of Turbulent Shear Flows’. *Adv. Geophys.* **18 A**, 224–236.
- Perry, A. E., S. M. Henbest, and M. S. Chong: 1986, ‘A Theoretical and Experimental Study of Wall Turbulence’. *J. Fluid Mech.* **165**, 163–199.
- Perry, A. E., K. L. Lim, and S. M. Henbest: 1987, ‘An Experimental Study of the Turbulence Structure in Smooth- and Rough-Wall Boundary Layers’. *J. Fluid Mech.* **177**, 437–466.
- Piomelli, U. and E. Balaras: 2002, ‘Wall-Layer Models for Large-Eddy Simulations’. *Ann. Rev. Fluid Mech.* **34**, 349–374.
- Piomelli, U., J. Ferziger, and P. Moin: 1989, ‘New Approximate Boundary Conditions for Large Eddy Simulations of Wall-Bounded Flows’. *Phys. Fluids A* **1**(6), 1061–1068.
- Pope, S. B.: 2000, *Turbulent Flows*. Cambridge University Press. 771 pp.

- Porté-Agel, F., C. Meneveau, and M. B. Parlange: 2000, 'A Scale-Dependent Dynamic Model for Large-Eddy Simulations: Application to a Neutral Atmospheric Boundary Layer'. *J. Fluid Mech.* **415**, 261–284.
- Rajagopalan, S. and R. A. Antonia: 1979, 'Some Properties of the Large Structure in a Fully Developed Turbulent Duct Flow'. *Phys. Fluids* **22**, 614–622.
- Saddoughi, S. G. and S. V. Veeravalli: 1994, 'Local Isotropy in Turbulent Boundary Layers at high Reynolds Number'. *J. Fluid Mech.* **268**, 333–372.
- Schlichting, H.: 1979, *Boundary-Layer Theory*. McGraw-Hill. 817 pp.
- Schumann, U.: 1975, 'Subgrid Scale Model for Finite Difference Simulations of Turbulent Flows in Plane Channels and Annuli'. *J. Comp. Phys.* **18**, 376–404.
- Stull, R. B.: 1988, *An Introduction to Boundary Layer Meteorology*. Kluwer. 670 pp.

Address for Offprints: St. Anthony Falls Laboratory
2 3rd Ave. SE
55414 Minneapolis, MN
U.S.A.